Acta Geotechnica (2007) 2:87–96
DOI 10.1007/s11440-007-0028-x

RESEARCH PAPER

Extreme pressure due to expanded cylindrical and spherical cavity in a limitless medium: applications in soil mechanics

Mounir Bouassida · Wissem Frikha

Received: 8 March 2006 / Accepted: 13 April 2007 / Published online: 14 July 2007

Abstract The extreme net pressure resulting from an expansion in a cylindrical or spherical cavity within a limitless medium is studied. Performing the static and kinematic approaches of yield design theory, analytical solutions of the extreme net pressure are established for cohesive–frictional as well as for purely cohesive medium. In the case of a cylindrical cavity, the identification between the analytical extreme net pressure and limit net pressure leads to the prediction of shear strength characteristics of soil. As useful result, in soil mechanics, the assessment of correlations using pressuremeter data has been discussed. Also, some assumptions for designing foundations, from pressuremeter data, have been highlighted.

Keywords Cavity expansion · Extreme net pressure · Kinematic approach · Pressuremeter test · Static approach · Yield design theory

List of symbols

a	radius of cavity
c_U	undrained cohesion
c	cohesion
$\underline{\underline{d}}$	tensor of strain rate
f	function defined the strength criterion
$G(\underline{x})$	domain of admissible stress fields
K	set of all potentially safe loads
K_a	coefficient of active pressure
p^*_{net}	extreme net pressure
p_0	lateral pressure at rest
p	pressure in the cavity
p^{mes}_{net}	limit net pressure measured from pressuremeter test
p^{mes}	limit pressure measured from pressuremeter test
$P_{déf}(\underline{v})$	power of deformation
$P_{ext}(\underline{v})$	power of external loads
$\underline{Q}$	vector of loading parameters
$\underline{\dot{q}}$	vector of kinematic parameters
r	radial distance from the centre of cavity
R	radius of influence zone
U	radial velocity expansion at the border of cavity
$\underline{v}$	velocity field displacement
$\underline{\underline{\sigma}}$	stress field
σ_r	radial stress
σ_θ	tangential stress
α	normalized radius
ϕ	angle of friction

M. Bouassida (✉) · W. Frikha
Ecole Nationale d'Ingénieurs de Tunis,
BP 37 Le Belvédère, 1002 Tunis, Tunisia
e-mail: mounir.bouassida@enit.rnu.tn

W. Frikha
e-mail: wissem.frikha@enit.rnu.tn

1 Introduction

The problem of cylindrical cavity expansion within a limitless half space was initially investigated by Lamé [20]. In this investigation, the soil surrounding the cavity, obeying to linear elastic behaviour, was assumed to be weightless, homogeneous, and isotropic.

It is quite difficult to quote all works which dealt with the study of the expanded cylindrical or a spherical cavity in an infinite medium. However, it can be envisaged to classify these works according to the type of each

contribution, i.e. analytical methods, numerical or experimental ones and others. The analytical methods have been developed by assuming various constitutive laws of the medium around the cavity, linearly elastic [20], elastic perfectly plastic without taking into account the volume variation [8, 12, 13, 22], or with volume variation [6, 17, 19, 21, 23, 26, 29, 31]. The main purposes of these contributions were the determination of mechanical characteristics of soils from pressuremeter or piezocone data and the prediction of bearing capacity of deep foundations. The analytical contributions were, adopting for the soil behaviour under two hypotheses: whether in small strains [5, 12, 13, 22, 29, 30], or with large strains [6, 8, 31].

Otherwise, it can also be mentioned that many researches dealt with the problem of cavity expansion, particularly for the pressuremeter test in relationship with the type of soil. In the case of purely cohesive soils the investigations have been done by [1, 3, 14, 15, 16, 18, 19, 25, 28]. While for a purely frictional soil the main contributions have been proposed by [9, 10, 21]. Furthermore, [6, 11, 22], have made specific proposals for cohesive–frictional soils.

In this paper, based on approaches of yield design theory, an analytical calculation of the extreme net pressure of a cylindrical and a spherical cavity, subjected to a radial expansion occurring in a limitless half space, is carried out. For this purpose, the notion of the radius of influence, referred to as the area where the state of stress is not negligible, is introduced. As application, a method is proposed for predicting the strength characteristics of soils.

Based on the similarity between the loading exerted by rigid foundations, which results in the stress bulbs, and that resulting from cylindrical cavity expansion, the prediction of the radius of influence enhances the depth where settlement might be calculated. Indeed, the method of settlement estimation performed by Menard [2] requires the calculation of deformation modulus for soil layers beneath the foundation up to eight times the foundation's breadth. Such depth estimation needs to be highlighted for a better comprehension of settlement calculation from pressuremeter data.

The problem of expanded cavity is undertaken by assuming small strain hypothesis which complies with the fixed geometry assumption adopted in yield design theory (YDT) [27].

Then, by identifying between the measured limit net pressure (from pressuremeter data) and the extreme net pressure, an estimation of the radius of influence around a cylindrical cavity is deduced. A method of prediction of strength characteristics for purely cohesive and cohesive–frictional soils is proposed.

Assessment of usual correlations, enabling the prediction of mechanical characteristics from pressuremeter data, is finally discussed.

2 Yield design theory (YDT)

The YDT generally aims at the determination of loadings which cause failure of structures. Such a problem is based on the compatibility between equilibrium and strength capacities of the constitutive material of a structure Ω subjected to a given loading process. As a result, the set (denoted by K) of all potentially safe loads of Ω is determined. Especially, loadings belonging to the border of K are called extreme load, which theoretically represent the exact solutions of failure loadings.

The set K can be conveniently built by performing the static approach, also called "from the inside". This approach permits to calculate lower bounds of the extreme load after solving a maximization problem with respect to parameters involved in the considered stress field [27].

The use of the principle of virtual work makes it possible to derive a formulation based upon the construction of kinematically admissible (K.A.) velocity fields. Such a kinematic approach, also called "from the outside", permits to derive upper bounds of the extreme load.

Combining the static and kinematic approaches, a bounding of the border of the set K is obtained [27].

For any K.A. velocity field and any statically admissible (S.A.) stress field, by using the principle of virtual works, equilibrium of Ω is:

$$\forall \underline{\underline{\sigma}}\ \text{S.A.}, \forall \underline{v}\ \text{K.A.}, \quad \mathrm{P}_{\mathrm{ext}}(\underline{v}) = P_{déf}(\underline{v}) \tag{1}$$

$P_{\mathrm{ext}}(\underline{v})$ = the power of external forces, in the case of a weightless medium, is:

$$P_{\mathrm{ext}}(\underline{v}) = \int_{\partial\Omega} \underline{T}(\underline{x}).\underline{v}(\underline{x})\mathrm{d}s = \underline{Q} \cdot \underline{\dot{q}}(\underline{v}) \tag{2}$$

$\underline{T}$ = the stress vector
$\partial\Omega$ = the boundary of Ω.

$\underline{Q}$ and $\underline{\dot{q}}(\underline{v})$ are, respectively, the vector of loading parameters (in the given loading process) and the vector of its associated kinematic parameters.

The constitutive material of Ω is governed by its strength criterion, denoted by $G(\underline{x})$,which is usually determined from experiments. $G(\underline{x})$ represents, in the space of Cauchy stress tensor components, the limitation of allowable stresses. This domain of allowable stress fields will be characterised by the property $\underline{\underline{\sigma}}(\underline{x}) \in G(\underline{x}) \quad \forall \underline{x} \in \Omega \quad \Leftrightarrow \quad \mathrm{f}\left(\underline{\underline{\sigma}}\right) \leq 0.$

For a cohesive–frictional material Coulomb's strength criterion is adopted. It is given by:

$$f\left(\underline{\underline{\sigma}}\right) = \underset{i,j=1,2,3}{\text{Sup}} \left\{\sigma_i(1+\sin\varphi) - \sigma_j(1-\sin\varphi) - 2c\cos\varphi\right\} \leq 0 \tag{3a}$$

i,j: denote the principal directions.

While for a purely cohesive material, Tresca's strength criterion is adopted. It corresponds to the particular case $\phi = 0$, then from Eq. (3a), it comes:

$$f\left(\underline{\underline{\sigma}}\right) = \underset{i,j=1,2,3}{\text{Sup}} \left\{\sigma_i - \sigma_j - 2c_U\right\} \leq 0 \tag{3b}$$

$c_U =$ the undrained cohesion.

In the following, the convention of positive tensile stresses, currently adopted in continuum mechanics, is adopted. Also G($\underline{x}$) will be simply denoted G.

A given loading Q is called "potentially safe" through the property [27]:

$$\begin{aligned} &\exists \underline{\underline{\sigma}} \text{ S.A. with Q} \\ &\text{and} \qquad\qquad \Leftrightarrow \text{Q} \in \text{K} \\ &\forall \underline{x} \in \Omega,\ \underline{\underline{\sigma}}(\underline{x}) \in G \end{aligned} \tag{4}$$

By using the kinematic approach with restriction to continuous velocity fields, the power of deformation is:

$$P_{déf}(\underline{v}) = \int_{\Omega} \underline{\underline{\sigma}}(\underline{x}) : \underline{\underline{d}}(\underline{x}) \mathrm{d}\Omega \tag{5}$$

$\underline{\underline{d}}(\underline{x}) =$ the strain rate tensor which components are calculated from the constructed K.A. velocity field as:

$$\underline{\underline{d}}(\underline{x}) = \frac{1}{2}\left[\frac{\partial v_i}{\partial x_j} + \frac{\partial v_j}{\partial x_i}\right] \tag{6}$$

Let introduce the $\pi\left[\underline{x}, \underline{\underline{d}}(\underline{x})\right]$ function defined by:

$$\pi\left[\underline{x}, \underline{\underline{d}}(\underline{x})\right] = \text{Sup}\left\{\underline{\underline{\sigma}}(\underline{x}) : \underline{\underline{d}}(\underline{x}), \underline{\underline{\sigma}} \in G\right\} \tag{7a}$$

For a cohesive–frictional soil, obeying to strength criterion given by Eq. (3a), the corresponding $\pi\left[\underline{x}, \underline{\underline{d}}(\underline{x})\right]$ function is:

$$\pi\left[\underline{x}, \underline{\underline{d}}(\underline{x})\right] = (c\,\text{cotg}\,\varphi) tr\underline{\underline{d}} \tag{7b}$$

If

$$tr\underline{\underline{d}} \geq (|d_1| + |d_2| + |d_3|)\sin\varphi \tag{7c}$$

$tr\underline{\underline{d}}$ = the first invariant of the strain rate tensor.

For a given continuous velocity field $\underline{v}$, the calculation of maximum resisting power is done when the state of stress $\underline{\underline{\sigma}}$ traverses all the domain G, then from Eqs. (5) and (7a) one obtains:

$$P(\underline{v}) = \int_{\Omega} \pi\left[\underline{x}, \underline{\underline{d}}(\underline{x})\right] \mathrm{d}\Omega \tag{8}$$

An upper bound of the set K is determined by applying the kinematic theorem stated as:

$$\underline{Q} \in K \Rightarrow \quad \forall\, \underline{\text{v}}\ K.A. \quad \underline{\text{Q}}.\underline{\dot{q}}(\underline{v}) \leq \text{P}(\underline{\text{v}}) \tag{9}$$

The best upper bound estimate of the extreme load will be determined after minimization of Eq. (9) with respect to the parameters involved in the constructed velocity field $\underline{v}$.

3 Expanded cylindrical cavity

3.1 Statement of the problem

Consider a limitless half space made up of a soil which is assumed as a homogeneous and isotropic medium. Consider, in such a medium a cylindrical cavity of radius a subjected to a radial expansion under pressure $p > p_0$ (Fig. 1).

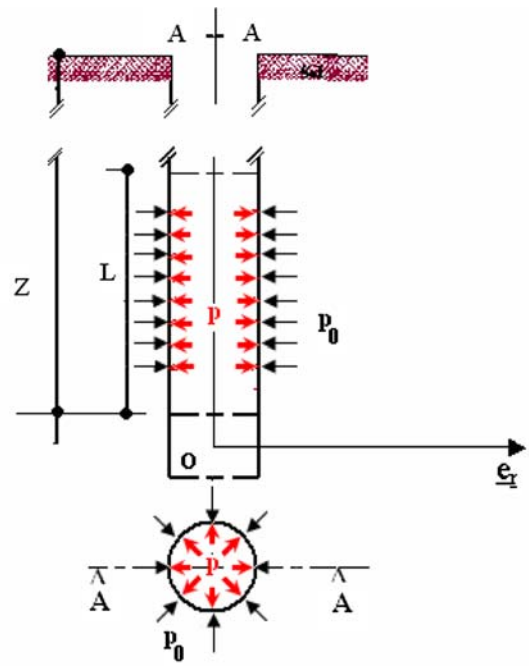

Fig. 1 Expansion of a cylindrical cavity

Due to geometrical and loading symmetries around the vertical axis (Oz) of the cavity (Fig. 1) the problem will be undertaken in polar co-ordinates (r, θ), as a plan strain study, where both radial and angular directions ($\underline{e}_r$ and $\underline{e}_\theta$) are considered as principal.

A smooth contact is assumed along the interface between the cavity and the half space. p_0 represents the initial horizontal stress at rest before the execution of cavity. Then the boundary conditions are given by:

along the border ($r = a$):

$$\sigma_r(r=a) = -p^*_{\text{net}} = -(p - p_o) \tag{10}$$

The velocity displacement vanishes at infinity:

$$r \to \infty \quad \underline{v} = \underline{0} \tag{11}$$

p, p_0 and p^*_{net} take positive values. p^*_{net} = the net pressure that represents the unique loading parameter. From Eq. (2), the associated kinematic parameter for p^*_{net} is:

$$\dot{q}(\underline{v}) = \int_{r=a} v_r(r=a)\ \mathrm{d}s = U \int_{r=a} \mathrm{d}s = 2\pi\ a\ U \tag{12}$$

With v_r $(r = a) = U > 0$, U = the radial velocity of expansion along the border $r = a$.

From Eqs. (2) and (12), the power of external forces is:

$$P_{\text{ext}}(\underline{v}) = p^*_{\text{net}}\, U\, 2\pi\, a \tag{13}$$

The static and kinematic approaches of yield design theory are undertaken, in the case of a cohesive–frictional material, to establish the extreme net pressure for expanded cylindrical cavity as well as for spherical cavity. The case of purely cohesive material is also treated.

3.2 Lower bound estimate of the extreme net pressure

Consider the family of two zones stress fields sketched in Fig. 2. Stress components depend solely on r variable, then:

$$a \le r \le R \quad \underline{\underline{\sigma}}(r) = \sigma_r(r)\underline{e}_r \otimes \underline{e}_r + \sigma_\theta(r)\underline{e}_\theta \otimes \underline{e}_\theta \tag{14}$$

$$r \ge R \quad \underline{\underline{\sigma}} \cong 0$$

R = the radius of zone (I) in which the radial stress σ_r and consequently, the state of stress is dominant. It is assumed the cavity expansion does not generate any significant stress component in zone (II).

For the statically admissible (S.A.) stress field $\underline{\underline{\sigma}}$ described by Eq. (14), equilibrium equations reduce to:

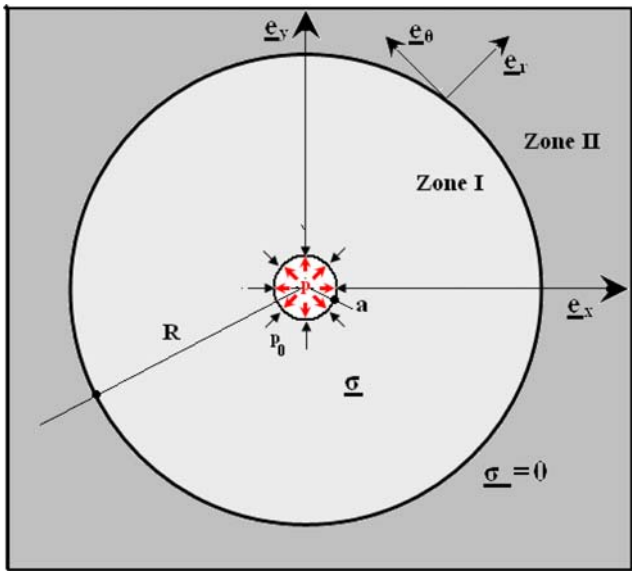

Fig. 2 The stress field with two zones

$$\frac{d\sigma_r}{dr} + \frac{\sigma_r - \sigma_\theta}{r} = 0 \tag{15}$$

Because the radial stress takes negative values (radial compression), from boundary condition in Eq. (10) when the radius increases from r = a it vanishes towards zero at infinite, then we have: $\frac{d\sigma_r}{dr} \ge 0$, therefore Eq. (15) leads to:

$$\sigma_r - \sigma_\theta \le 0 \tag{16}$$

The constructed stress field should comply with Coulomb's strength criterion given by Eq. (3a). Then, solving Eq. (15) under conditions (3a) and (16) leads to:

$$\sigma_r \le c\,\mathrm{cotg}\ \varphi \left[1 - \left(\frac{r}{R}\right)^{K_a - 1}\right] \tag{17}$$

$K_a = tg^2\left(\frac{\pi}{4} - \frac{\varphi}{2}\right)$ denotes the coefficient of active pressure.

Substituting Eq. (10) into Eq. (17) the lower bound estimate of extreme net pressure is:

$$p^*_{net} \ge c\,\mathrm{cotg}\ \varphi \left[\left(\frac{a}{R}\right)^{K_a - 1} - 1\right] \tag{18}$$

In the case of a purely cohesive material, making use of the same procedure, detailed above, for cohesive–frictional material, the radial stress which complies with Tresca's strength criterion (3b) is:

$$\sigma_r \le 2c_U \mathrm{Ln}\left(\frac{r}{R}\right) \tag{19}$$

Therefore, from Eqs. (10) and (19), the lower bound of extreme net pressure is:

$$p^*_{\text{net}} \geq 2\, c_U \,\text{Ln}\left(\frac{R}{a}\right) \tag{20}$$

3.3 Upper bound estimate of the extreme net pressure

The case of a cohesive–frictional medium (c ≠ 0 and $\phi \neq 0$) is considered. The kinematically admissible (K.A.) velocity field, defined by:

$$\underline{v} = U\left(\frac{r}{a}\right)^{-K_a} \underline{e}_r \tag{21}$$

is exhibited.

According to Eq. (6), from Eq. (21), the strain rate tensor is:

$$\underline{\underline{d}} = U\,\frac{r^{-K_a-1}}{a^{-K_a}}\left(-K_a \underline{e}_r \otimes \underline{e}_r + \underline{e}_\theta \otimes \underline{e}_\theta\right) \tag{22}$$

then from Eq. (22), the first invariant of the strain rate tensor is:

$$tr\underline{\underline{d}} = (1 - K_a)U\frac{r^{-K_a-1}}{a^{-K_a}} \tag{23}$$

and

$$|d_1| + |d_2| + |d_3| = (1 + K_a)U\frac{r^{-K_a-1}}{a^{-K_a}} \tag{24}$$

After Eqs. (23) and (24), the condition in (7c) is fulfilled. Then, substituting Eq. (23) in Eq. (7b) it comes:

$$\pi\left(\underline{x}, \underline{\underline{d}}(\underline{x})\right) = c\,\text{cotg}\;\varphi(1 - K_a)U\frac{\mathrm{r}^{-K_a-1}}{a^{-K_a}} \tag{25}$$

The maximum resisting power follows from Eq. (13) as:

$$P(\underline{\mathrm{v}}) = \frac{2\pi U}{a^{-K_a}}\mathrm{c}\;\mathrm{cotg}\varphi\left(R^{1-K_a} - a^{1-K_a}\right) \tag{26}$$

Substituting Eqs. (13) and (26) in Eq. (9), the upper bound of the extreme net pressure is:

$$p^*_{\text{net}} \leq c\,\text{cotg}\;\varphi\left[\left(\frac{a}{R}\right)^{K_a-1} - 1\right] \tag{27}$$

The case of a purely cohesive medium ($c_U \neq 0$ and $\phi = 0$) is addressed by substituting $K_a = 1$ in Eq. (21), the velocity field is:

$$\underline{v} = U\left(\frac{a}{r}\right)\underline{e}_r \tag{28}$$

This kinematically admissible (K.A.) velocity field should comply with condition $tr\underline{\underline{d}} = 0$, provides a finite maximum resisting power [27]. The π function introduced in Eq. (7a) is:

$$\pi\left(\underline{x}, \underline{\underline{d}}(\underline{x})\right) = c_U\left(\left|-U\left(\frac{a}{r^2}\right)\right| + \left|U\left(\frac{a}{r^2}\right)\right|\right) = 2\, c_U\, U\left(\frac{a}{r^2}\right) \tag{29}$$

Then, from Eqs. (28) and (29), the maximum resisting power is:

$$P(\underline{v}) = 4\pi c_U U\, a\text{Ln}\left(\frac{R}{a}\right) \tag{30}$$

Substituting Eqs. (13) and (30) in Eq. (9), the upper bound of extreme net pressure is:

$$p^*_{\text{net}} \leq 2\, c_U \text{Ln}\left(\frac{R}{a}\right) \tag{31}$$

3.4 Combination of the static and kinematic approaches

According to lower and upper bounds established respectively from the static and kinematic approaches of YDT, the extreme net pressure p^*_{net} is derived. In the case of cohesive–frictional medium ($c \neq 0$ and $\phi \neq 0$) from Eqs. (18) and (27), it comes:

$$p^*_{\text{net}} = c\,\text{cotg}\;\varphi\left[\left(\frac{R}{a}\right)^{1-K_a} - 1\right] \tag{32}$$

In the case of purely cohesive material, ($c_U \neq 0$ and $\phi = 0$) from Eqs. (20) and (31) the extreme net pressure is:

$$p^*_{\text{net}} = 2\, c_U \text{Ln}\left(\frac{R}{a}\right) \tag{33}$$

It should be noted when the friction angle ϕ tends towards zero, the extreme net pressure given by Eq. (33) is easily deduced from Eq. (32).

Using the theorem of "association" [27], the stress field defined by Eqs. (14), (15), (17) and (19), and velocity fields expressed by Eqs. (21) and (28), are called associated. For such a situation, the maximum resisting power given by Eq. (8) equals the power of external forces given by Eq. (13), in which the extreme net pressure is substituted by Eq. (32) in case of cohesive–frictional medium, or by Eq. (33) in the case of purely cohesive medium.

4 Expanded spherical cavity

4.1 Statement of the problem

Consider a spherical cavity (with radius a) subjected to a radial expansion under pressure $p > p_0$. The determination

of extreme net pressure, using YDT approaches, is conducted by adopting the same procedure as for an expanded cylindrical cavity. Calculations are carried out for cohesive–frictional as well as for purely cohesive medium.

Consider the following stress field expressed in the principal spherical coordinates system (r, θ, ϕ):

$$a \le r \le R \quad \underline{\underline{\sigma}}(r) = \sigma_r(r)\,\underline{e}_r \otimes \underline{e}_r + \sigma(r)\left(\underline{e}_\theta \otimes \underline{e}_\theta + \underline{e}_\phi \otimes \underline{e}_\phi\right) \tag{34}$$

$$r \ge R \quad \underline{\underline{\sigma}} \cong 0$$

Due to symmetrical loading and geometry, for any S.A. stress field $\underline{\underline{\sigma}}$, equilibrium equations reduce to:

$$\frac{d\sigma_r}{dr} + 2\,\frac{\sigma_r - \sigma}{r} = 0 \tag{35}$$

4.2 Lower bound estimate of the extreme net pressure

Consider the case of a cohesive–frictional medium ($c \neq 0$ and $\phi \neq 0$). The compatibility between equilibrium according to Eqs. (38) and (16) and Coulomb's strength criterion (3a), leads to:

$$\sigma_r \le c\,\mathrm{cotg}\;\varphi\left[1 - \left(\frac{r}{R}\right)^{2(K_a-1)}\right] \tag{36}$$

R = the radius of the zone of influence.

Taking account of Eq. (36) and boundary condition (10) the lower bound estimate of extreme net pressure is:

$$p^*_{\mathrm{net}} \ge c\,\mathrm{cotg}\varphi\left[\left(\frac{a}{R}\right)^{2(K_a-1)} - 1\right] \tag{37}$$

For a purely cohesive medium, making use of the same procedure, as detailed for a cohesive–frictional material, the radial stress which complies with Tresca's strength criterion (3b) is:

$$\sigma_r \le 4c_U \mathrm{Ln}\left(\frac{r}{R}\right) \tag{38}$$

Then, the corresponding lower bound estimate of the extreme net pressure is:

$$p^*_{net} \ge 4c_U \mathrm{Ln}\left(\frac{R}{a}\right) \tag{39}$$

4.3 Upper bound estimate of the net extreme pressure

Consider the kinematically admissible (K.A.) velocity field, defined by:

$$\underline{v} = U\left(\frac{r}{a}\right)^{-2K_a}\underline{e}_r \tag{40}$$

$U > 0$ is the radial velocity expansion along the border ($r = a$) of a spherical cavity.

Such a velocity field complies with condition (7c) to derive a finite maximum resisting power. Using the same procedure, as detailed for the case of cylindrical cavity (Eqs. 22–25), from Eqs. (8) and (40), it comes:

$$P(\underline{v}) = \frac{4\pi \mathrm{U}}{a^{-2K_a}}\,c\,\mathrm{cotg}\;\varphi\left(R^{2(1-K_a)} - a^{2(1-K_a)}\right) \tag{41}$$

From Eq. (2) the power of external forces is:

$$P_{\mathrm{ext}} = \int_{r=a} p^*_{\mathrm{net}} U dS = p^*_{\mathrm{net}} U 4\pi a^2 \tag{42}$$

Substituting Eqs. (41) and (42), in Eq. (9), the upper bound of the extreme net pressure is:

$$p^*_{\mathrm{net}} \le c\,\mathrm{cotg}\;\varphi\left[\left(\frac{a}{R}\right)^{2(K_a-1)} - 1\right] \tag{43}$$

The case of a purely cohesive medium ($c_U \neq 0$, $\phi = 0$) is considered by substituting $K_a = 1$ in Eq. (40), the velocity field is:

$$\underline{v} = \mathrm{U}\left(\frac{a}{r}\right)^2 \underline{e}_r \tag{44}$$

This K.A. velocity field which complies with condition $tr\underline{\underline{d}} = 0$ provides a finite maximum resisting power. After calculation, making use of the kinematic theorem, the upper bound of the extreme net pressure is:

$$p^*_{\mathrm{net}} \le 4\,c_U \mathrm{Ln}\left(\frac{R}{a}\right) \tag{45}$$

According to upper and lower bounds, established from the static and kinematic approaches of YDT, the expression of extreme net pressures are identified by combining Eqs. (37) and (43) for a cohesive–frictional and Eqs. (39) and (45) for a purely cohesive medium, it follows:

$$c \neq 0;\varphi \neq 0 \qquad p^*_{\mathrm{net}} = c\,\mathrm{cotg}\;\varphi\left[\left(\frac{R}{a}\right)^{2(1-K_a)} - 1\right] \tag{46}$$

$$c_U \neq 0;\varphi = 0 \qquad p^*_{\mathrm{net}} = 4\,c_U\,Ln\left(\frac{R}{a}\right) \tag{47}$$

After the theorem of association [27], the stress fields and velocity fields constructed for expanded spherical cavity are called associated.

5 Illustration for expanded cylindrical cavity

When coring undisturbed sample (in soft soil, for instance) reveals impossible to carry out laboratory tests, the strength characteristics of soils can be predicted from pressuremeter data.

From the pressuremeter test (as well as from in situ tests) the parameters of soils are usually determined at each meter depth. Such an advantage leads to a better knowledge of soil characteristics, especially in the case of thick layers.

The pressuremeter test is carried out in a cylindrical borehole during which an increase of radial pressure results from the expansion of the pressuremeter cell. Recorded measurements are water pressure and the volume variation of the pressuremeter cell [4]. The pressuremeter test is conducted until failure which is characterized either by a variation of volume of soil equals twice the initial cell volume, or a quasi-constant pressure of expansion. As a result, three characteristics are determined: the Ménard modulus and the limit pressure p^{mes} and pressure at rest p_0. [4, 7]. Then the limit net pressure is deduced by: $p_{\text{net}}^{\text{mes}} = p^{\text{mes}} - p_0$.

The soil behaviour, around an expanded cell of pressuremeter, was discussed by Nahra and Frank [24] based on finite element computation. It was concluded, particularly, that stress components become negligible beyond a distance ranging from 25 to 50 times the radius of pressuremeter cell. Figure 2 illustrates (zone I) this radius of influence witch depends on the adopted constitutive model for the soil around the cavity. Therefore, the radius of influence, denoted R, is interpreted as the distance from which the radial stresses, as well as other stress components, resulting from the expanded cavity are neglected. The normalized radius of influence is, then, introduced as ratio $\alpha = R/a$.

Nahra and Frank [24] and Fawaz et al. [10] discussed the choice of radius R by performing finite element computations. It was agreed, the value $\alpha = 14$ is suitable for studying the soil behaviour around an expanded cylindrical cavity.

5.1 Illustration and discussions of results

Consider, first, the case of a purely cohesive soil. Substituting in Eq. (33) the value of limit net pressure $p_{\text{net}}^{\text{mes}}$ by the extreme net pressure p_{net}^{*} established from YDT approaches, therefore, the cohesion of soil is:

$$c_U = \frac{p_{\text{net}}^{\text{mes}}}{2\,Ln\left(\frac{R}{a}\right)} \tag{48}$$

Figure 3 shows an asymptotic evolution of the normalized radius plotted as a function of the normalized pressure

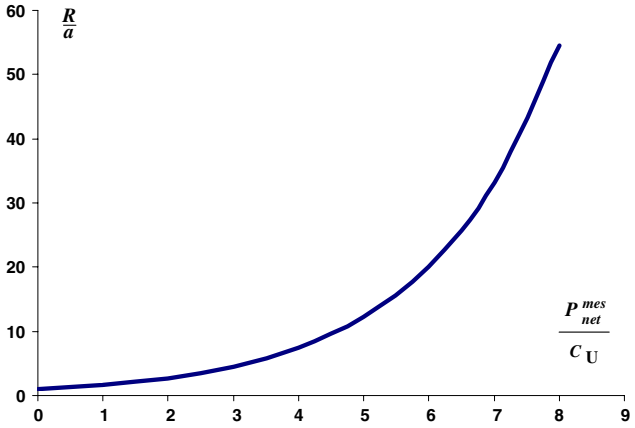

Fig. 3 Normalized radius $\alpha = \left(\frac{R}{a}\right)$ as a function of the normalized pressure $\left(\frac{p_{\text{net}}^{\text{mes}}}{c_U}\right)$ for a purely cohesive soil

$\left(\frac{p_{\text{net}}^{\text{mes}}}{c_U}\right)$. It can be noted that the choice of $\alpha = 30$ is quite sufficient for predicting the undrained cohesion. As first estimation, from Fig. 3, we have $\alpha = 7p_{\text{net}}^{\text{mes}}$. Also, from Fig. 4 it is clearly shown that for $\alpha = 15$, as suggested by Fawaz et al. [10], a good prediction of the undrained cohesion from the measured limit net pressure is deduced. Such a prediction is usually representative for soft soils in terms of values of limit net pressure, it is:

$$c_U = \frac{p_{\text{net}}^{\text{mes}}}{5.4} \tag{49}$$

The prediction of undrained cohesion from Eq. (49) is also in good agreement with the correlation proposed by the "Centre of Ménard" studies for the case of soft clays i.e.:$c_U = \frac{p_{\text{net}}^{\text{mes}}}{5.5}$ Amar and Jézéquel [1]. This correlation was proposed from a large experimental data base.

In the case of a cohesive–frictional medium, by equalling the extreme net pressure (YDT) to the measured limit

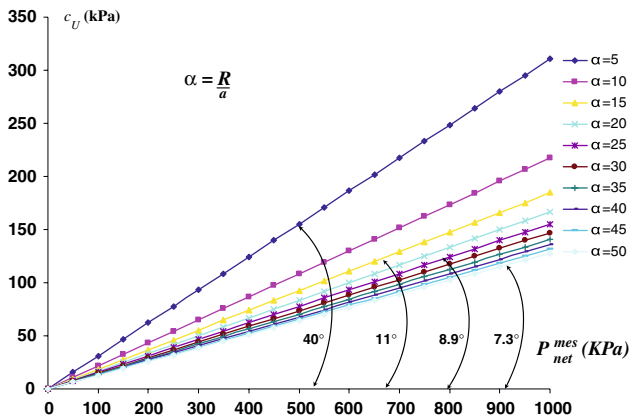

Fig. 4 Undrained cohesion against extreme net pressure for $\alpha = 5$–50

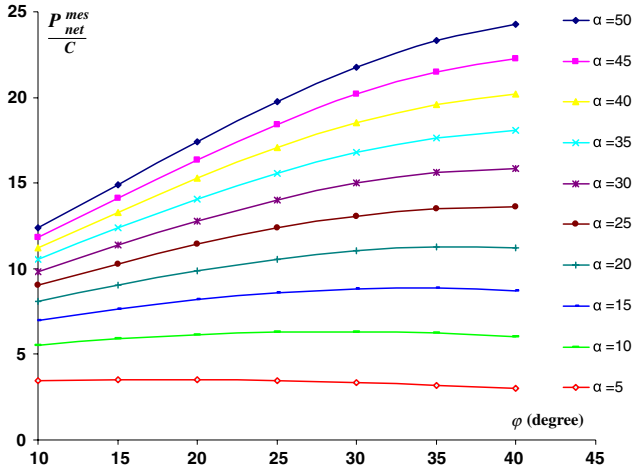

Fig. 5 Normalized radius α against normalized pressure $\left(\frac{p_{net}^{mes}}{c}\right)$ as a function of angle of friction

net pressure (pressuremeter test), from Eq. (32), the cohesion and the angle of friction are obtained as a function of the normalized limit net pressure and the normalized radius α:

$$\frac{p_{net}^{mes}}{c} = \text{cotg}\varphi\left(\alpha^{1-K_a} - 1\right) \tag{50}$$

Figure 5 shows the significant influence of the normalized radius when predicting the limit net pressure. Nevertheless, it should be noted that, in the range $10 \le \alpha \le 15$, a quasi-constant limit net normalized pressure can be predicted for

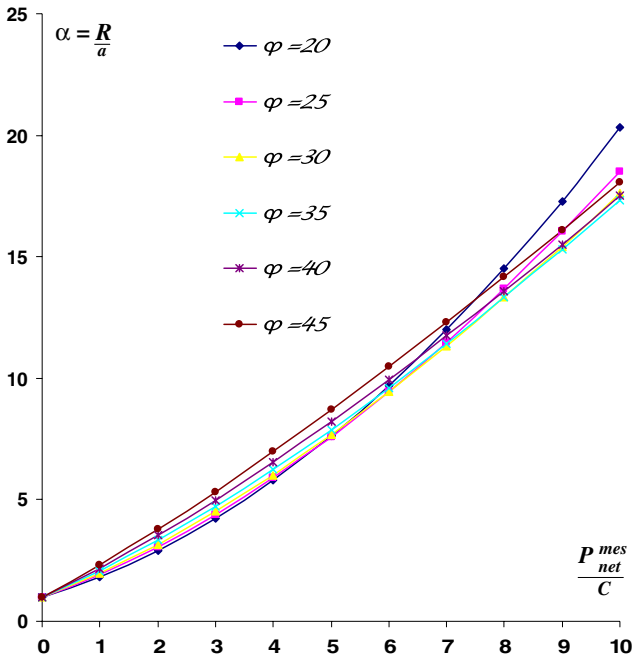

Fig. 6 Normalized radius $\left(\frac{R}{a}\right)$ as a function of the normalized pressure $\left(\frac{p_{net}^{mes}}{c}\right)$ for a cohesive–frictional soil

Table 1 Values of functions F and F_e for different values of the angle of friction ϕ

ϕ (°)	5	10	15	20	25	30	35	40	45
$F(\phi)$	6.21	6.97	7.63	8.18	8.57	8.80	8.86	8.73	8.43
F_e (ϕ)	6.13	7.01	7.71	8.22	8.56	8.74	8.78	8.69	8.51

representative values of the friction angle ($10° \le \varphi \le 40°$). This result is also well illustrated in Fig. 6.

Consider, then, the value of normalized radius α = 15 in Eq. (50), the mechanical characteristics of a cohesive–frictional material are simply predicted by:

$$\frac{p_{net}^{mes}}{c} = F(\varphi) \tag{51}$$

Using a first order approximation of the function F (ϕ), an equivalent expression is deduced:

$$F_e(\varphi) = \left(-11.93(\sin\varphi)^2 + 13.32\sin\varphi + 5.06\right) \tag{52}$$

Table 1 compares between the functions given by Eqs. (51) and (52) for a wide range of the friction angle. Figure 7 shows a good agreement between Functions $F(\phi)$ and F_e (ϕ). Then, it is possible to write:

$$p_{net}^{mes} = c\left(-11.93(\sin\varphi)^2 + 13.32\sin\varphi + 5.06\right) \tag{53}$$

As a result, the recorded limit net pressure from the pressuremeter test is identified with the extreme net pressure (established from yield design theory), makes it possible to estimate the strength characteristics of soil at failure (c and ϕ), and the radius of influence of an expanded cylindrical cavity.

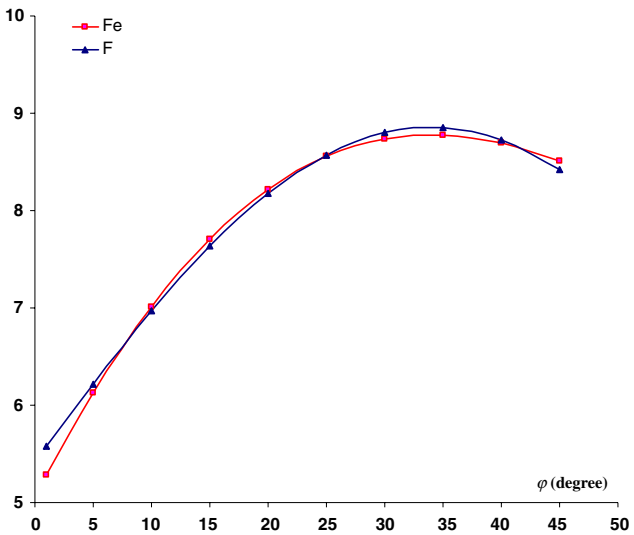

Fig. 7 Functions $F(\phi)$ and F_e (ϕ)

5.2 Prediction of strength characteristics

Consider the value of normalized radius $\alpha = 15$. It roughly corresponds to the ratio between the depth on which settlement is estimated by Ménard's method [22] and the radius of a circular foundation (or half width of a rectangular foundation). In other words the depth along which a significant settlement of soil is expected also corresponds to the radius of influence R limiting the zone where stress and strains are significant.

The strength characteristics of a given soil, for which the measured limit net pressure is given from pressuremeter test, can be predicted by two methods.

Firstly, for a given soil the value of the angle of friction might be estimated. For example, consider a silty clay from the area of Rades-La Goulette (Tunisia), starting from a geotechnical investigation recorded characteristics (pressuremeter and classical triaxial tests), $p_{\text{net}}^{\text{mes}} = 200$ kPa, $c = 25$ kPa and $\phi = 16°$. From Fig. 8, for $\phi = 16°$ and the corresponding iso-values curve of limit net pressure $p_{\text{net}}^{\text{mes}} = 200$ kPa, the cohesion is c = 25.8 kPa. Such a prediction of soil cohesion shall be made more accurately from typical chart as shown in Fig. 9.

Secondly, from Fig. 10, consider the same silty clay for which the friction angle is about of 16°, the corresponding normalized limit net pressure i.e. $\frac{p_{\text{net}}^{\text{mes}}}{c} = 7.75$ is deduced from which follows the cohesion value: $c = 25.8$ kPa.

The proposed method of prediction will be conversely more suitable for a prior estimation of cohesion. In this case, the friction angle will be predicted directly from Fig. 9 for a given value of the limit net pressure recorded from the pressuremeter test. For example consider a sandy silt in the same zone, with limit net pressure $p_{\text{net}}^{\text{mes}} = 400$ kPa, if assuming $c = 60$ kPa, the predicted friction angle is $\phi = 22°$.

Finally, the proposed method of prediction requires some experience when adopting the value of first strength characteristic of soils, either the friction angle or the cohesion. The predicted value of the second characteristic obviously depends on the reliability of the pressuremeter data.

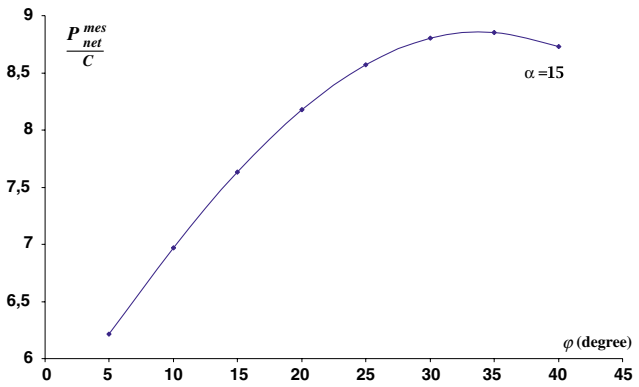

Fig. 8 Normalized pressure as a function of angle of friction ϕ for $\alpha = 15$

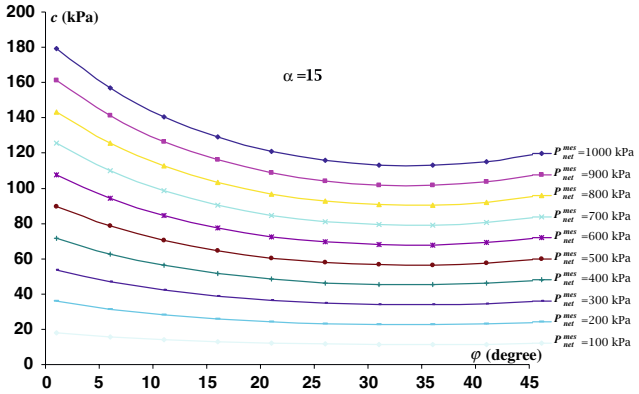

Fig. 9 Cohesion versus of angle of friction ϕ for iso-values of net limit pressure for $\alpha = 15$

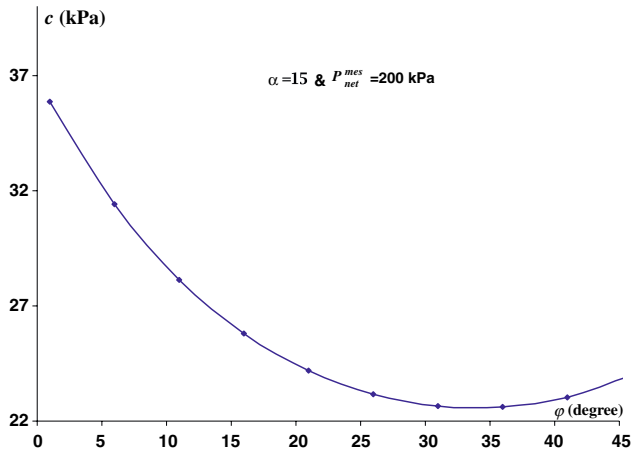

Fig. 10 Cohesion versus the angle of friction ϕ for $p_{\text{net}}^{\text{mes}} = 200$ kPa and $\alpha = 15$

6 Conclusion

Based on yield design theory approaches, this study has focused on the theoretical determination of the extreme net pressure which results from lateral expansion exerted, within an infinite half-space, in cylindrical as well as spherical cavity.

Linking between the recorded limit net pressure from the pressuremeter data and the theoretical predictions, the radius of influence of expanded cylindrical cavity is estimated.

Such estimation complies with previous values suggested from the study by finite element on the soil behaviour around an expanded cavity.

Based on the estimated radius of influence, the assessment of usual correlations has been discussed especially for soft soils assumed as purely cohesive medium. Also, the depth along which the settlement is predicted based on pressuremeter standard has been assessed.

These findings well illustrate a comprehensive handling of soil characteristics, to be predicted from the pressuremeter data for design purposes in soil mechanics.

Useful charts were proposed for cohesive–frictional soils to estimate the cohesion as well as the friction angle from pressuremeter data. Conversely, if strength characteristics as results from laboratory tests are provided, the proposed method can be used to predict the assumed limit net pressure during a pressuremeter test to be performed in a given soil.

References

1. Amar S, Jézéquel JF (1972) Essais en place et en laboratoire sur sols cohérents, comparaisons des résultats. Bulletin de Liaison des Laboratoires des Ponts et Chaussées n°58, mars-avril, Paris, pp 97–108
2. Amar S, Clark BGF, Gambin MP, Orr TLL (1991) Utilisation des résultats des essais pressiométriques pour le dimensionnement des fondations en Europe. Rapport sur l'état des connaissances établies par le Comité Technique Européen de la SIMSTF, comité technique régional européen n°4, 1ère partie: pressiomètre Ménard et pressiomètre auto foreur, A.A. Belkema, pp 25–48
3. Anderson WF, Pyrah IC, Hajji Ali F (1987) Rate effects in pressuremeter tests in clays. J Geotech Eng Div ASCE 113(11):1344–1358
4. Baguelin F, Jézéquel JF, Shields DH (1978) The pressuremeter and foundation engineering. Series on rock and soil mechanics, vol 2 n°4, 1st edn. Trans. Tech. Publication
5. Bishop AW, Hill R, Mott M (1945) The theory of indentation and hardness tests. In: Proceedings of physical society, third part, n° 321, May
6. Carter JP, Booker JR, Yeung SK (1986) Cavity expansion in cohesive frictional soils. Géotechnique 36(2):349–358
7. Cassan M (1969) Les essais in situ en mécanique des sols. Revue Construction n° 7 et 8, juillet-août. Paris
8. Chadwick P (1959) The quasi-static expansion of a spherical cavity in metal and ideal soils. Part I. Quart J Mech App Math 12:52–71
9. Combarieu O (1996) A propos de la détermination de l'angle de frottement des sols pulvérulents au pressiomètre. Revue Française de Géotechnique n°77. 4ème trimestre. pp 51–57
10. Fawaz A, Biguenet G, Boulon M (2000) Déformations d'un sol pulvérulent lors de l'essai pressiométrique, Revue Française de Géotechnique n° 90. 1èr trimestre. pp 3–14
11. Gambin MP (1977) Le pressiomètre et la détermination de l'angle de frottement et de la cohésion d'un sol. Geoprojekt XXV Lat. Colloque de Halin, 26 Września
12. Gibson RE, Anderson WF (1961) In situ measurement of soil properties with the pressuremeter. Civil engineering and public works review, pp 615–661
13. Hill R (1950) The mathematical theory of plasticity. In: The expansion of a spherical shell. Clarendon, Oxford
14. Houlsby GT, Carter JP (1993) The effects of pressuremeter geometry on the results of tests in clay. Geotechnique 43(4):567–576
15. Huang AB, Chameau JL, Holtz RD (1986) Interpretation of pressuremeter data in cohesive soils by simplex algorithm. Technical note. Géotechnique 36(4):599–603
16. Huang AB, Holtz RD, Chameau JL (1991) Laboratory study of pressuremeter tests in clays. J Geotech Engin Div ASCE 117(10): 1549–1567
17. Hughes JMO, Worth CP, Windle D (1977) The pressuremeter test in sands. Géotechnique 27(4):455–472
18. Jang In Sung, Chung Choong-Ki, Kim Myoung Mo, Cho Sung Min (2003) Numerical assessment on the consolidation characteristics of clays from strain holding, self-boring pressuremeter test. Comput Geotech 30(2):121–140
19. Ladanyi B (1963) Expansion of a cavity in saturated clay medium. J Soil Mech Foundations Div Am Soc Civil Eng 89(SM 4):127–161
20. Lamé G (1852) Leçons sur la théorie mathématique de l'élasticité des corps solides. Bachelier, Paris
21. Manassero B (1989) Stress–strain relationships from drained self-boring pressuremeter test in sands. Géotechnique 39(2):293–307
22. Ménard L (1957) Mesures in situ des propriétés physiques des sols. Annales des Ponts et Chaussées. Mai-Juin
23. Mecsi J (1991) Stresses, displacements, volume changes around the expansion cylinder in the soil. In: Proceedings of 10th European conference on soil mechanics and foundation engineering, Florence, 26–30 May V1, pp 243–246. Balkema, Rotterdam
24. Nahra R, Frank R (1986) Contribution numérique et analytique de l'étude de la consolidation autour du pressiomètre. Rapport de Recherche Laboratoire Central des Ponts et Chaussées. n° 137
25. Palmer AC (1972) Undrained plane strain expansion of a cylindrical cavity in clay: a simple interpretation of a pressuremeter test. Géotechnique 22(3):451–457
26. Salençon J (1966) Expansion quasi-statique d'une cavité à symétrie sphérique ou cylindrique dans un milieu élastoplastique. Annales des Ponts et Chaussées -III- mai juin, pp 175–187
27. Salençon J (1990) An introduction to the yield design theory and its applications to soil mechanics. Eur J Mech A Solids 9(5):477–500
28. Thevanayagam S, Chameau JL, Altschaeffl AG (1994) Some aspects of pressuremeter test interpretation in clays. Geotechnique 44(2):319–334
29. Vesic AS (1972) Expansion of cavities in infinite Soil Mass. J Soil Mech Foundations Div Am Soc Civil Eng 22(3):451–457
30. Wroth CP, Windle D (1975) Analysis of the pressuremeter test allowing for volume change. Géotechnique 25(3):589–604
31. Yu HS, Houlsby GT (1991) Finite cavity expansion in dilatant soils: loading analysis. Géotechnique 41(2):173–183